International Journal of Surface Engineering and Interdisciplinary Materials Science
Volume 11 • Issue 1

Developing Self-Cleaning Photocatalytic TiO_2 Nanocomposite Coatings

Jean Claude Mallia, University of Malta, Malta
Anthea Agius Anastasi, University of Malta, Malta
Sophie Marie Briffa, University of Malta, Malta*

ABSTRACT

Photocatalytic coatings with self-cleaning properties are becoming increasingly more popular due to the increased awareness of the importance of cleaning and the associated high cost of cleaning supplies and services. This research investigated self-cleaning photocatalytic polydimethylsiloxane (PDMS)/ titanium dioxide (TiO_2) nanocomposite coatings and focused on selecting the optimal TiO_2 phase and concentration. To date, the comparison of the different TiO_2 phases as a nanocomposite coating has not been sufficiently considered. PDMS/TiO_2 nanocomposite coatings with three nanomaterial (NM) samples (an anatase, rutile, and mixed phase) and three concentrations of TiO_2 (0.6, 1 and 3 w/v%) were prepared, applied to glass slides by dip coating, and tested with respect to hydrophobicity, surface stability, antifogging, and photocatalytic properties. It was found that a stable hydrophobic coating with the optimal photocatalyitc performance was produced with 3 w/v% anatase TiO_2.

KEYWORDS

Hydrophobic, Nanocomposite, Photocatalytic Coating, Polydimethylsiloxane, Self-Cleaning, Titanium Dioxide Nanomaterials

INTRODUCTION

Surface coatings are often used to improve or introduce desired properties onto substrates of components in many industries such as the food (Aresta et al., 2013; Singh et al., 2017), cosmetic (Dréno et al., 2019), automotive (Ali et al., 2016; Coelho et al., 2012; Shafique & Luo, 2019), medical (Nasimi & Haidari, 2013; Rai et al., 2019), environmental (Pathakoti et al., 2018), electronics (Magdassi et al., 2010), and marine (Silva-Bermudez & Rodil, 2013; Tong et al., 2022) industries. Lately, advanced photocatalytic and hydrophobic surface coatings are being developed due to the desirable self-cleaning and antifogging properties which can be beneficial in many applications such as solar cells, windows (Adachi et al., 2018; Lan et al., 2013; Syafiq et al., 2018; Zhao & Lu, 2021), and optical lenses and in the automotive industry (Chemin et al., 2018).

DOI: 10.4018/IJSEIMS.324757 *Corresponding Author

The self-cleaning ability of coatings can be a result of hydrophobicity (Banerjee et al., 2015; Benedix et al., 2000). Hydrophobic surfaces have low wettability, and contact angles of water droplets are around 100° or greater. When relying on hydrophobicity, self-cleaning coatings provide the benefit of reducing cleaning costs and conserving time and water due to the lotus leaf effect they create (Benedix et al., 2000; Rios et al., 2009). Presently, water scarcity is detrimentally affecting billions of people, and as such, water conservation is quickly becoming an international priority, with it being currently the 11th Sustainable Development Goal set out by the United Nations.

Hydrophobic surfaces can also contribute to high-performance antifogging properties. Antifogging coatings improve the optical performance of products since the substrate is always left optically clear (Chemin et al., 2018). Since the property of antifogging is achieved by having a coating with a surface tension that prevents the formation of stagnant water and water bubbles on a surface, the two properties of self-cleaning and antifogging can be achieved together with superhydrophobic coatings (Garlisi & Palmisano, 2017). Common drawbacks of current antifogging coatings include their limited lifetime, increased surface tension over time which leads to higher surface contamination, and a low surface stability (Chemin et al., 2018).

Besides hydrophobicity, photocatalysis can also result in the self-cleaning of surfaces (Fujishima et al., 2008; Nakata & Fujishima, 2012; Parkin & Palgrave, 2005; Ragesh et al., 2014). When photocatalytic semiconductors such as titanium dioxide (TiO_2), zinc oxide (ZnO), and nickel oxide (Moura & Picão, 2022) are irradiated with ultraviolet (UV) light, "electron-hole" pairs are formed and the holes cause oxidation whilst the electrons form the reduction system. From oxidation, hydroxyl radicals are created from oxidised hydroxide (OH^-) and water molecules. From the reduction system, peroxyl groups are generated from the dioxygen (O_2) found in the atmosphere (Bourikas et al., 2014; Jang et al., 2001; Lan et al., 2013). These hydroxyls and peroxyl groups, termed as reactive oxygen species (ROS), give rise to self-cleaning effects which degrade both organic and inorganic matter into safe compounds such as carbon dioxide and water (Bourikas et al., 2014; Jang et al., 2001; Lan et al., 2013; Tavares et al., 2014). Materials such as TiO_2 obtain photocatalytic effects in the nanometric range due to the high surface area to volume ratio (Strauss et al., 2014). These smaller sized nanomaterials (NMs) exhibit better photocatalytic effects (Moura & Picão, 2022; Wang et al., 2019) since the energy needed by the charge carriers is proportional to the NM size (Lan et al., 2013; Wang et al., 2019).

TiO_2 has the ability of heterogeneous photocatalysis, whereby TiO_2 in the solid state reacts with media which are in either the liquid or the gas state (Kumar et al., 2021; Yasmina et al., 2014) and therefore can have self-cleaning capabilities (Garlisi & Palmisano, 2017; Imran et al., 2015; Nam et al., 2019; Panutumrong et al., 2015; Syafiq et al., 2018; Yasmina et al., 2014). Jang et al. (2001) studied the photocatalytic properties of TiO_2 nanoparticles using methylene blue dye and found that the photocatalytic ability was inversely proportional to NM size and directly proportional to anatase fraction of a mixed phase sample. Furthermore, TiO_2 NMs provide benefits over other photocatalytic semiconductors including their low toxicity, high recyclability, and great chemical stability which makes them desirable for practical applications (Haider et al., 2019; Linden & Mohseni, 2014; Racovita, 2022; Shafaamri et al., 2020; Wang et al., 2019).

Research suggests that the phase composition of the TiO_2 can have an influence on the photocatalytic behaviour of the final coating and thus should be taken into consideration (Jang et al., 2001; Lan et al., 2013; Sakthivel et al., 2006). TiO_2 has three phases – anatase, rutile, and brookite – each of which has specific behaviour and properties (Racovita, 2022). The anatase and rutile phases are more commonly used in research due to the pair being the cheapest, more abundantly found, and most effective photocatalysts (Linden & Mohseni, 2014; Shafaamri et al., 2020; Wang et al., 2019). Furthermore, most research accepts that the anatase phase has the best photocatalytic performance (Augustynski, 1993; Jain & Vaya, 2017; Jang et al., 2001; Lan et al., 2013; Tayade et al., 2007). However, some research has found that a mixed phase of both anatase and rutile can lead to higher photocatalytic performance (Farbod & Khademalrasool, 2011). For example, while investigating the effect of particle size of synthesised TiO_2 NMs, it was found that a mixed phase TiO_2 NM with 71.5% of the phase being anatase and the rest rutile had the highest

photocatalytic performance (Farbod & Khademalrasool, 2011). However, limited research directly compares the photocatalytic behaviour of anatase and rutile TiO_2 NMs as part of nanocomposite coatings. Most of the research available to date compares the phases of TiO_2 NMs as powders and not as a coating for the purposes of photocatalytic nanocomposite coatings for optical performance.

TiO_2 as a NM component for photocatalytic smart nanocomposite coatings has shown promising results which can lead to self-cleaning effects (Garlisi & Palmisano, 2017; Imran et al., 2015; Nam et al., 2019; Panutumrong et al., 2015; Syafiq et al., 2018; Tavares et al., 2014) and overall better antifogging performance with higher coating stabilities (Garlisi & Palmisano, 2017). A promising bonding agent that can be used in conjunction with TiO_2 NMs is polydimethylsiloxane (PDMS). PDMS is a soft polymer. This makes it useful in processes such as coating, moulding, embossing, and stamping. In surface coatings, PDMS is a very effective bonding agent due to properties such as its chemical inertness and low interfacial free energy (Gale et al., 2016). This is a very useful since PDMS will not react with other chemicals or materials or shrink its area due to surface tensions (Coster, 2003). PDMS also has a very good thermal stability and optical transparency and can be modified with relative ease (Gale et al., 2016). PDMS coated glass substrate has been found to possess the optical transparency above 90% in the visible region and low refractive index at 1.52. Furthermore, PDMS coatings possess high hydrophobicity and excellent self-cleaning properties after two-month outdoor exposure (Syafiq et al., 2019). PDMS coated glass substrate possesses good adhesion with maximum load 1200 mN, strong durability, and great anti-fog properties (Syafiq et al., 2019).

Syafiq et al. (2018) showed that when compared to uncoated glass, PDMS/TiO_2 nanocomposite surface coatings with a 3.33 wt% TiO_2 concentration on glass substrates provided self-cleaning effects as the coating removed any residue or dirt from its surface and showed superior antifogging properties due to the high surface energy of the surface coating. Wang et al. (2019) showed that a superhydrophobic PDMS/TiO_2 nanocomposite coating also proved to have effective self-cleaning performance when carrying out the methylene blue test. Furthermore, Wang et al. (2019) showed that this coating had very good environmental stability against UV, heat, and rainfall and had good corrosion resistance. However, none of these studies explore the optimal TiO_2 phase and loading concentration in nanocomposite coatings.

In this work, photocatalytic PDMS/TiO_2 nanocomposite surface coatings on glass slides were developed with the aim of determining the best phase composition of TiO_2 NMs and effective loading concentration to be used in PDMS/TiO_2 nanocomposite coatings. The investigation focused on the selection of the most ideal TiO_2 nanomaterials phase and concentration to obtain the optimal self-cleaning properties along with sufficient optical clarity and coating homogeneity.

MATERIALS AND METHODS

Materials

Three TiO_2 NMs each having different phases were obtained from the European Commission Joint Research Centre; the rutile phase (JRCNM62002a), the anatase phase (JRCNM10202a), and a mixed phase sample containing both anatase and rutile (JRCNM01005a). SYLGARD 182 PDMS prepolymer and a curing agent, obtained from Farnell Limited, were used to produce the PDMS binding agent. Methylene blue dye used for photocatalytic testing was purchased from LEVO laboratory Services Ltd. Ethanol with a purity of 99.9% (denatured with 10 ppm Bitrex) was used as a solvent and for cleaning along with acetone (Pure Grade) and distilled water. All solvents were supplied from Chemic Ltd.

Methods

Characterisation of Pristine Particles

Pristine NM powders were characterised by means of X-ray diffraction (XRD) and scanning electron microscopy (SEM). XRD was carried out using a Rigaku Ultima IV with a copper source with a

voltage of 40 kV and a current of 40 mA. The scan ranged between 10° and 90° with a scan speed of 1°/min. The crystalline phase data was extracted and compared to Data Base (DB) cards obtained from the PDXL 2 software.

Samples were imaged with a Carl Zeiss Merlin 42-16 Gemini II column field emission scanning electron microscope. An electron high tension voltage of 8 kV, a working distance of 5.6 mm, and a magnification range from 20k to 500k were implemented. Image J software was used to measure the size of individual NMs. Three-hundred NMs were measured for each sample to obtain the size distribution curves.

Coating Fabrication

The glass slides (26 × 76 × 1 mm) from MASTERGLASS were first cleaned with distilled water, followed by acetone and finally ethanol by ultrasonication for 10 minutes in each solvent. The glass slides were then dried with nitrogen gas.

Each TiO_2 NM (rutile, anatase, and mixed sample) was first added to the PDMS curing agent and ultrasonicated for 30 minutes. The final PDMS solution was prepared by mixing 10 parts of the PDMS prepolymer with one part of the PDMS curing agent containing the dispersed TiO_2 NMs. Three different final concentrations of 0.6, 1, and 3 w/v% TiO_2 were used. This was left to degas in a vacuum chamber set at 0.2 bar for 45 minutes.

The glass samples were coated with the nanocomposite coating by dip coating using a ACEdip 2.0 dip coater by SOLGELWAY. Initially, multiple combinations of dip coating parameters (immersion speed, withdrawal speed, and holding time), as listed in Table 1, were tried and tested to obtain the most consistent, defect free, and thin coating.

Coated samples were immediately cured in an oven at a temperature of 150 °C for 20 minutes. The curing involved hanging the glass slide vertically (i.e., having the same orientation as for dip coating). The resultant coatings were investigated for optical clarity, coating consistency, and coating uniformity, with each of these properties being given a qualitative ranking, as described in Table 2. The dip coating parameters were modified until all three qualitative properties reached the desired quality.

Table 1. Dip coating parameters tested

Test	Immersion Speed (mm/s)	Withdrawal Speed (mm/s)	Holding Time (s)
1	0.5	0.5	60
2	0.4	0.4	60
3	0.4	0.4	100
4	0.4	0.2	100
5	0.3	0.2	100
6	0.2	0.2	100
7	0.2	0.1	100

Table 2. Qualitative ranking description for dip coating parameters tested

Rank	Description
X	A poor and unacceptable quality
O	An improved quality
√	A desirable quality

Following the ranking results, Table 3 shown in the results below, an immersion and withdrawal speed of 0.2 mm/s and 0.1 mm/s, respectively, and a holding time of 100s were chosen and used for dip coating of the slides for subsequent testing.

Control glass substrates coated with PDMS only were also produced in a similar manner. Furthermore, glass slides coated with TiO_2 NMs (1 w/v%) dispersed in ethanol were prepared to determine the wettability of TiO_2 NMs on their own.

Coating Analysis and Testing

Water contact angle (WCA) measurements were obtained using a DataPhysics OCA 15EC Instruments system and the SCA20 version 5.0.41 software. A dosing volume of 2 µL and dosing rate of 1 µL/s were used. Three repeated readings were obtained on three different slides. The resulting WCAs were then averaged. Measurements were repeated after samples were irradiated with UV light with a wavelength of 352 nm in an Opsytec Dr. Global UV-chamber Model 820 220 for 7 days. The intensity of UV exposure used was 4.4 times greater than that of sunlight to simulate an accelerated exposure.

Antifogging performance of the 0.6 w/v% samples was studied by leaving the samples in a freezer at a temperature of -25 °C for 2 hours. These were then taken out and exposed to a temperature of 18 °C and humidity of 76%. Samples were visually inspected after 15 minutes. UV-VIS spectroscopy was carried out using a Shimadzu SolidSpec-3700 DUV UV-VIS-NIR Spectrophotometer. As per ISO 10678-2010 standard (British Standards, 2017), the samples were immersed in methylene blue dye (20 µmol/L) and placed in the Opsytec Dr. Global UV-chamber Model 820 220. Absorbance measurements were taken at 664 nm. The test was run for 3 hours with readings taken at 30-minute intervals. Three repeats of each sample were performed to reduce uncertainty in the results. Furthermore, following the 7-day UV exposure, the durability of the nanocomposite coating containing the 3% wt/v anatase TiO_2 NMs was tested by measuring the photocatalytic performance observed by methylene blue decolourisation as described above.

RESULTS AND DISCUSSION

Characterisation of Pristine Particles

Phase Composition

The XRD results, shown in Figure 1, confirm the presence of the anatase, rutile, and anatase-rutile mixed phases in the TiO_2 NM samples. The anatase phase was confirmed by the main peak representing the (101) plane at $2\theta = 25.95°$. For the rutile sample, the main peak was represented by the (110) plane at $2\theta = 28.1°$. The final sample which consisted of both the anatase, and rutile phases showed peaks representative of both phases, with the two major peaks representing the (101) plane and the (110) plane at 2θ values of 25.95° and 28.1°, respectively, being detected. The fact that no shifts in 2θ values between the mixed sample and the single-phase sample were noted indicated that the mixed sample contained a physical mixture of phases and not a chemical mixture. Due to the relative peak intensities, the mixed sample seems to indicate that the majority of the phase composition was anatase.

Morphology

Electron microscopy revealed that the TiO_2 NMs were all rod-like in shape as seen in Figures 2-4 (a and b). This is beneficial for this type of coating as rod-like TiO_2 NMs have been reported to possess better optical properties than spheres (Liao & Liao, 2007). The average shortest and longest lengths of the TiO_2 NMs were all found to be in the region of c. 15 ± 5.56 and 40 ± 9.68 nm, respectively, as seen in Figures 2-4 (c and d). Since all three samples had a similar size and shape, any differences in the photocatalytic performance observed for the different NMs can be attributed solely to the different phase composition. This is an important consideration as both the size and the shape of nanoparticles have significant effects on the optical, electronic, and catalytic properties of TiO_2 NMs because of changes in surface area, number of active sites, and quantum size effect (Liao & Liao, 2007).

Figure 1. XRD diffractograms of samples compared with DB cards of the anatase, rutile, and anatase-rutile mixed phase

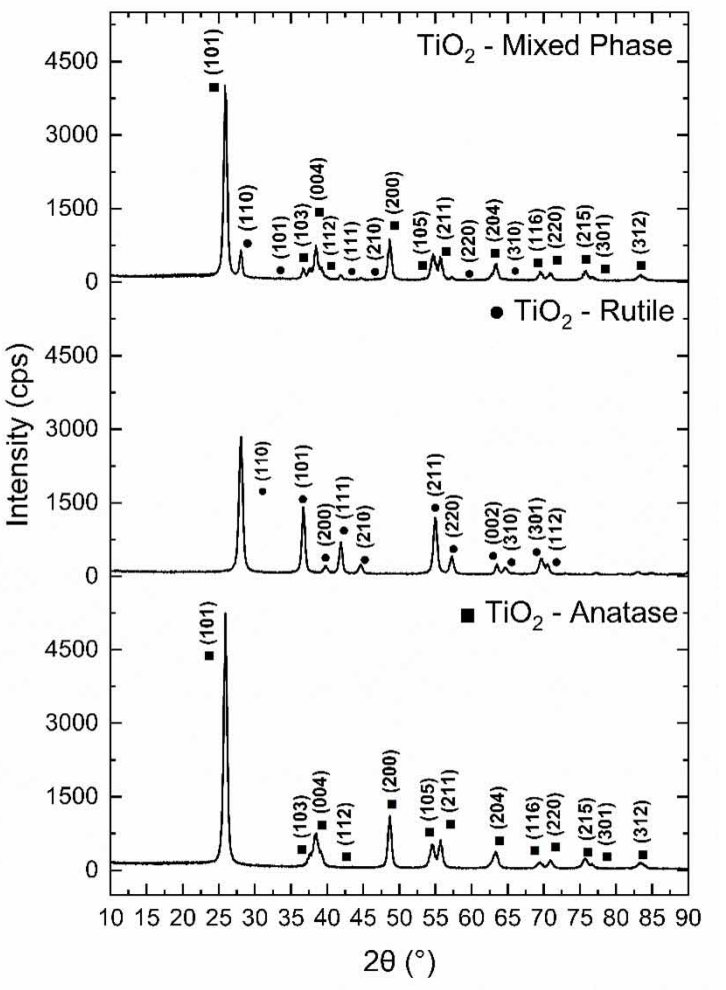

Coating Fabrication

The qualitative ranking for coating uniformity, optical clarity, and coating consistency given for the various dip coating parameters tested is shown in Table 3. As the immersion speed and withdrawal speed were decreased and the holding time was increased, the quality of the coating was observed to improve.

The slow withdrawal speed allows the glass slide to be withdrawn from the dispersion without disrupting the dynamic and static meniscus of the dispersion, hence improving the optical clarity and consistency – at faster speeds, turbulence is formed at the dynamic meniscus, producing gelled areas and resulting in a striped appearance (Shafaamri et al., 2020). Furthermore, greater immersion speeds also detrimentally affect the optical clarity and consistency, due to surface tension disruptions which lead to micro cracks and inconsistencies in the coating, as seen in Figures 5a and 5b. It was observed that the holding speed mostly affected the uniformity of the wet coating before curing. From these tests, to obtain the best uniformity, it was found that a relatively slow withdrawal speed must be accompanied with a long holding time. It is assumed that the dispersion had enough time to settle on glass slides and limited the possibility of turbulence as it was withdrawn. Hadi Yousefi et

Figure 2. SEM micrographs at a) low and b) high magnification, along with size distribution graphs for the c) longest and d) shortest lengths of the rutile TiO_2 NMs

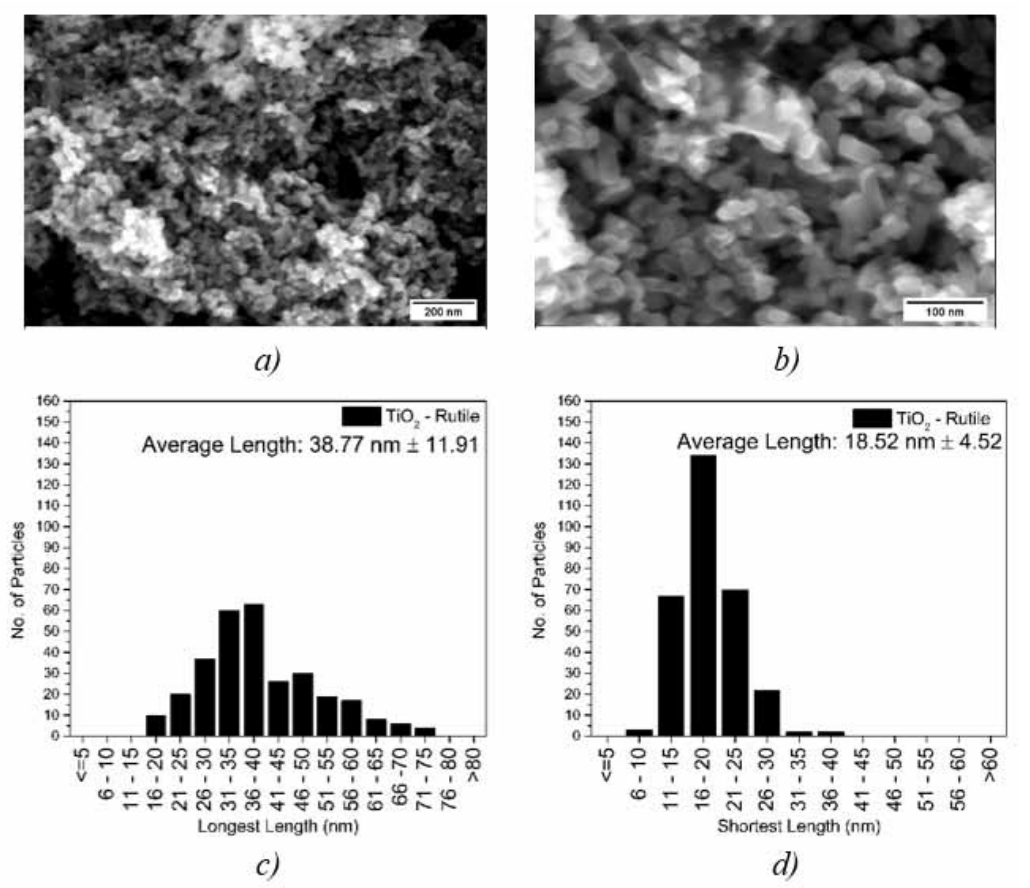

al. (2017) also found that a longer holding time creates a more stable coating when investigating the dip coating effect on the performance of alumina-PDMS nanofiltration membranes for desalination.

The best combination to obtain the desired properties of optical clarity, coating consistency, and coating uniformity, which were assessed visually, were found to be an immersion and withdrawal speed of 0.2 mm/s and 0.1 mm/s, respectively, with a holding time of 100s (i.e., Test 7), as seen in Figure 5c. The withdrawal speed and holding time settings were the instrument's limits.

Coating Analysis and Testing

Hydrophobicity

TiO_2 NMs (1 w/v%) on their own were found to be hydrophilic, as seen in Figure 6, as they had a WCA of less than 90° in agreement with the studies of Garlisi and Palmisano (2017) and Syafiq et al. (2018). The anatase sample had the lowest WCA. Vrakatseli et al. (2020) compared the WCA achieved by nano-TiO_2 film coatings with anatase and rutile phases. From their results it was also found that the anatase had the highest wettability. This could be due to the larger production of electron-hole pairs migrating to the surface of the TiO_2 NMs resulting in surface oxygen vacancies which lead to higher wettability. The mixed phase sample had a WCA value (50.06° ± 6.06°) between that of the rutile (65.68° ± 1.16°) and that of the anatase (44.13° ± 3.56°) sample.

Figure 3. SEM micrographs at a) low and b) high magnification, along with size distribution graphs for the c) longest and d) shortest lengths of the anatase TiO_2 NMs

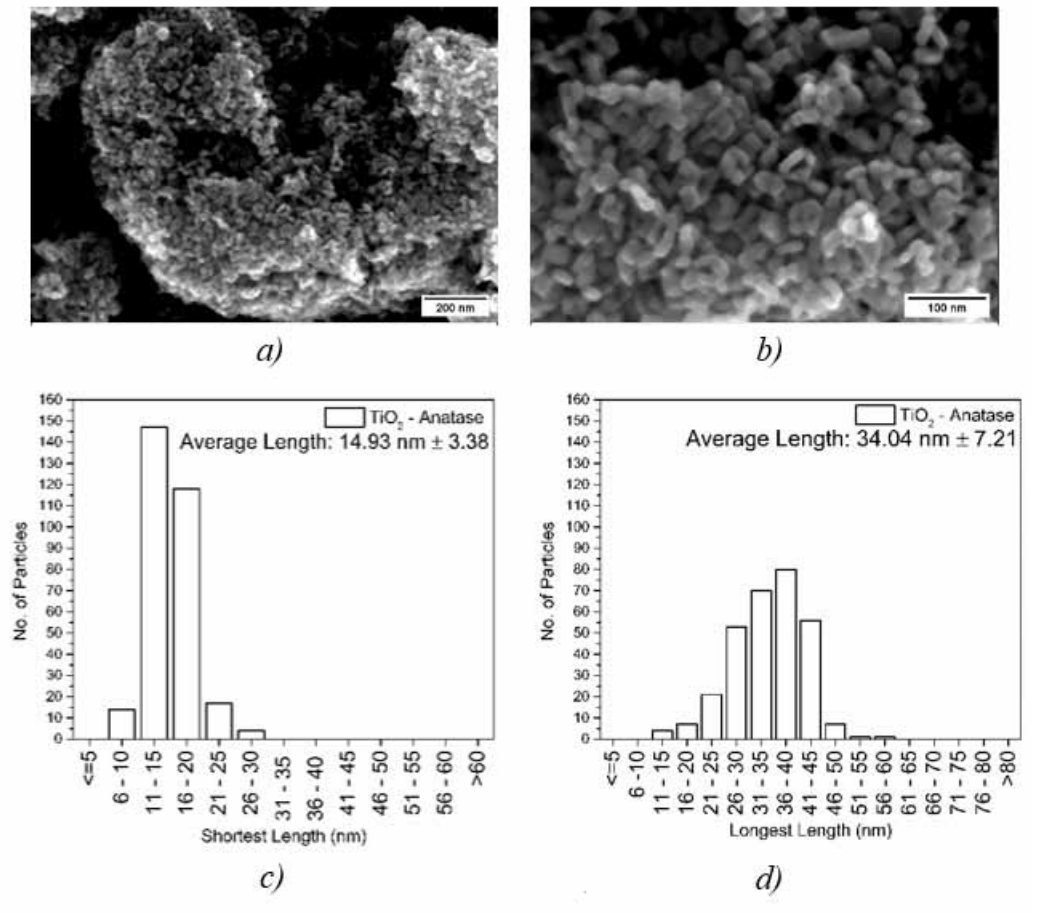

As shown in Figure 7, the PDMS coating alone had a WCA of around 110.78° ± 0.34°, indicating the hydrophobic nature of the surface due to the intrinsic high surface tension of the PDMS. This is also in agreement with the findings of Syafiq et al. (2019). Upon the addition of the otherwise hydrophilic TiO_2 NMs, the PDMS/TiO_2 coatings resulted in more hydrophobic surfaces with even higher WCA values, as seen in Figure 7. Although the TiO_2 phase composition did not seem to affect the degree of hydrophobicity of the PDMS/TiO_2 coatings to a significant degree, the mixed phase samples once again had average WCA values between those of the rutile and anatase samples for every TiO_2 concentration tested.

An increase in hydrophobicity was recorded upon increasing the TiO_2 concentration, as seen in Figure 7, with the samples loaded with 3 w/v% TiO_2, showing a significant increase in hydrophobicity compared to the lower concentrations. This was as a result of the increasing surface tension due to the higher loading of NMs, in agreement with the work of Kovacs and Vincett (1985), who showed that an increase in embedded particles led to an increase in surface tension and hence an increase in hydrophobicity.

Figure 4. SEM micrographs at a) low and b) high magnification, along with size distribution graphs for the c) longest and d) shortest lengths of the anatase-rutile mixed phase TiO_2 NMs

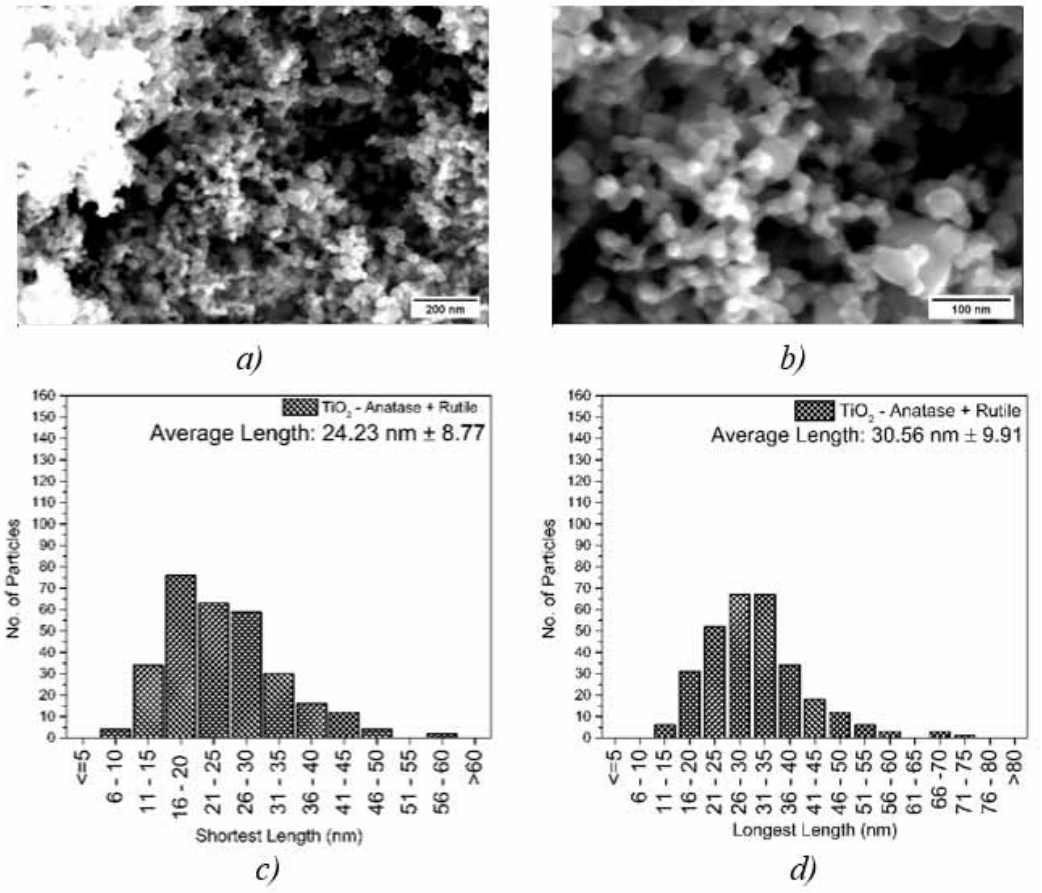

Table 3. Qualitative ranking given for coating uniformity, optical clarity, and coating consistency for dip coating parameters tested

Test	Coating Uniformity	Optical Clarity	Coating Consistency
1	X	O	X
2	X	O	X
3	O	O	X
4	O	O	O
5	√	O	O
6	√	√	O
7	√	√	√

Antifogging

To date, the performance of antifog property is measured by the visibility of fog droplets and evaporation time only (Meng et al., 2022; Syafiq et al., 2020). There are still no specific parameters

Figure 5. a) and b) show resulting Defects in the PDMS/TiO_2 nanocomposite coating whilst c) shows the desired quality coating (Test 7)

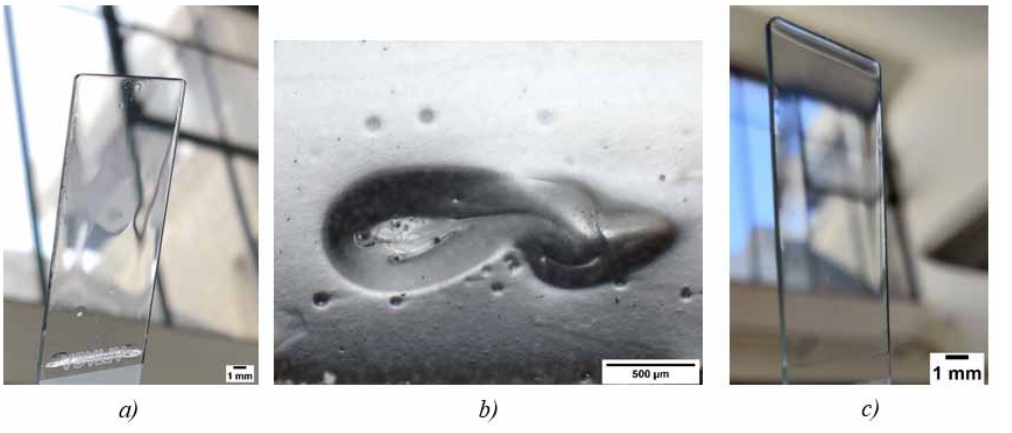

Figure 6. Average WCA measurement with error bars representing the standard deviation of TiO_2 NM samples

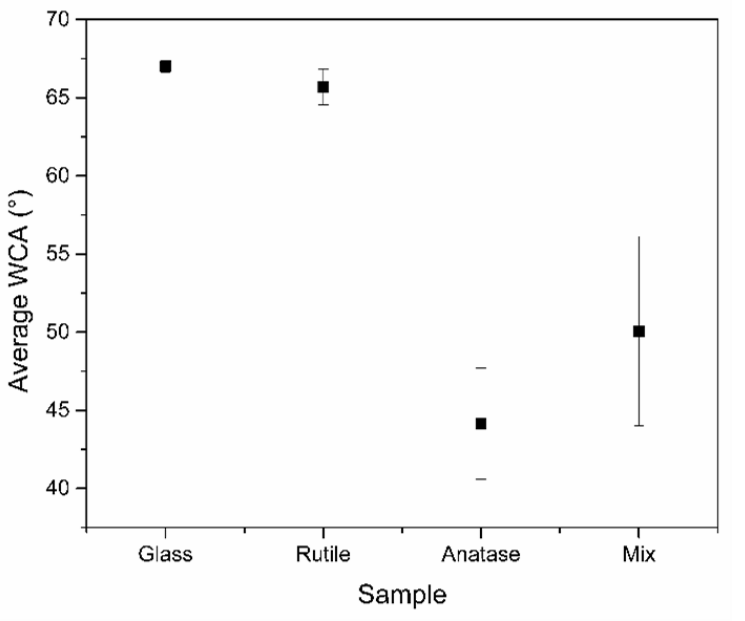

in measuring the visibility of foggy glass. All the PDMS coated samples showed good antifogging performance as the samples achieved optical clarity as evidenced by the lack of condensation on the surface within a short timeframe. Compared to the uncoated sample, which took longer than 15 minutes to dry up, the PDMS and PDMS/TiO_2 nanocomposite coated samples dried up in 2 minutes, as seen in Figure 8. The good antifogging performance is once again attributed to the high surface tension and hence hydrophobicity of the PDMS. Similar results to those shown in Figure 8 were reported with 3.33 wt% PDMS/TiO_2 nanocomposite coatings (Syafiq et al., 2018). The difference in the TiO_2 NMs phases did not influence the antifogging performance of the coatings.

Figure 7. Average WCA measurements of PDMS/TiO_2 nanocomposite coatings with increasing concentrations (0, 0.6, 1 & 3 w/v%)
Note. Error bars represent the standard deviation.

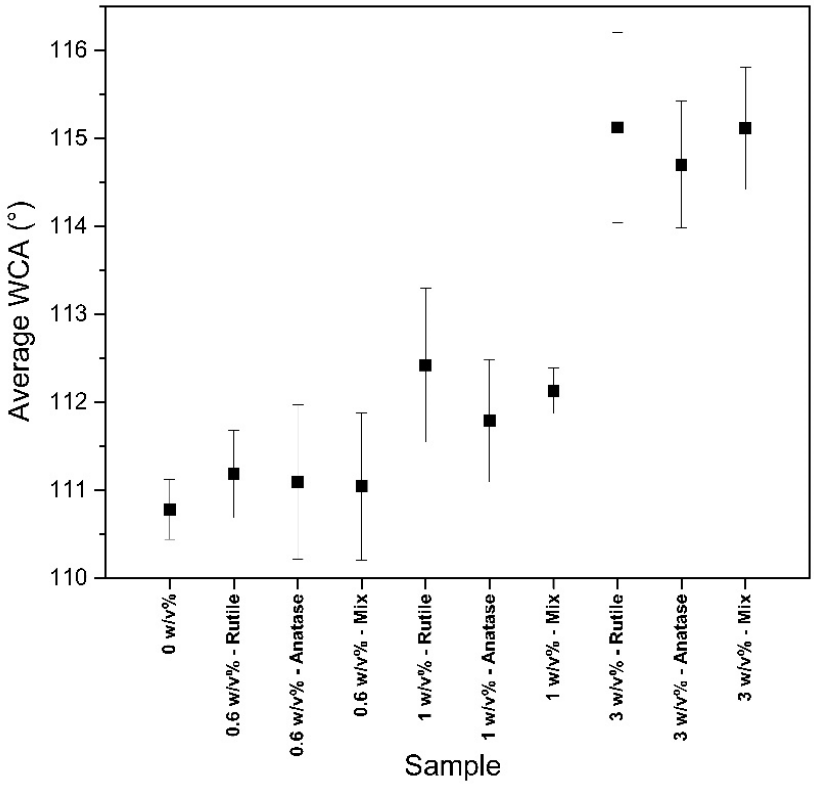

Figure 8. Antifogging testing showing a) PDMS/TiO_2 (mixed sample 0.6 w/v%) nanocomposite coating and b) uncoated glass slide after 15 minutes

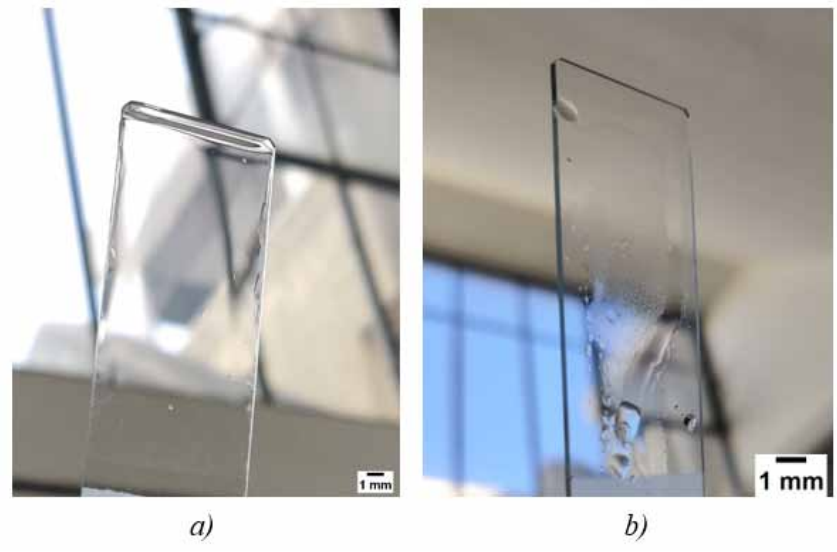

Photocatalytic Performance

UV-VIS spectroscopy was carried out to determine the photocatalytic activity of the PDMS/TiO_2 nanocomposite surface coatings. On comparing different concentrations (0, 0.6, 1, and 3 w/v%) of mixed phased TiO_2 NMs embedded in PDMS, it resulted that only the 3 w/v% showed enough photocatalytic performance to overcome the inhibition effect of the PDMS covering some of the TiO2 NMs, as seen in Figure 9. The lower concentration of 1 wt% PDMS/TiO_2 nanocomposite coating reported to exhibit satisfactory photocatalytic activity by Tavares et al. (2014) can be attributed to the fact that the PDMS used in their research was diluted with hexane and was spray coated, hence achieving thinner coatings.

Figure 10 presents the absorbance of methylene blue dye over time for each sample (anatase, rutile, and mixed phase) at a concentration of 3 w/v%. These graphs are also shown in Figure 13 in the Appendix along with the best decay curve fit. The results show that the anatase phase exhibited the greatest photocatalytic effect with a reduction in absorbance measurement by 5% after 180 minutes, as opposed to the rutile phase for which there was no marked reduction in the absorbance measurement. It is believed that the less prominent photocatalytic effect of the rutile phase was inhibited by the PDMS binding agent while the superior electronic structure of anatase (Jang et al., 2001) generated better charge carrier movement, resulting in greater amounts of ROS (Lan et al., 2013) that thus helped overcome the inhibition of the PDMS binding agent. The mixed sample indicated similar results and trends to the anatase loaded sample, as seen in Figure 13. Such similarities are attributed to its physical mixed phase composition and higher anatase fraction as deduced from the XRD results, as seen in Figure 13. Similar results were recorded for unbound TiO_2 NMs whereby the rate of decolourisation of methylene blue and hence the photocatalytic effect, were both less prominent with an increase in the rutile mass fraction (Jang et al., 2001).

Generally, it is thought that anatase is the phase with the better photocatalytic performance due to it having a Fermi level 0.1 eV greater than the rutile phase (Lan et al., 2013), the presence of an indirect bandgap in its electronic structure as opposed to the rutile phase which has a direct bandgap,

Figure 9. Absorbance of methylene blue at 664 nm over time for each different concentration of mixed phased TiO_2 NMs embedded in PDMS

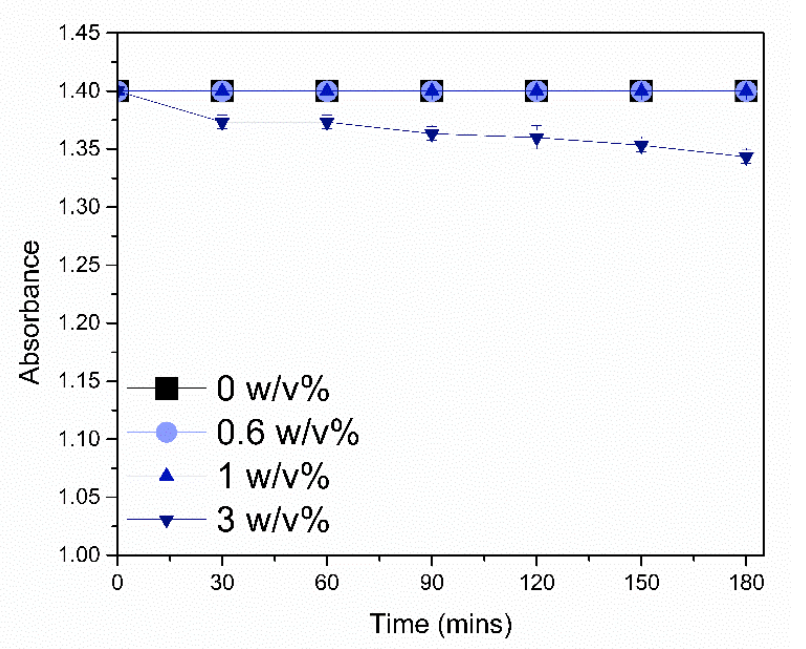

Figure 10. Absorbance of methylene blue at 664 nm over time for each PDMS/TiO_2 coated sample

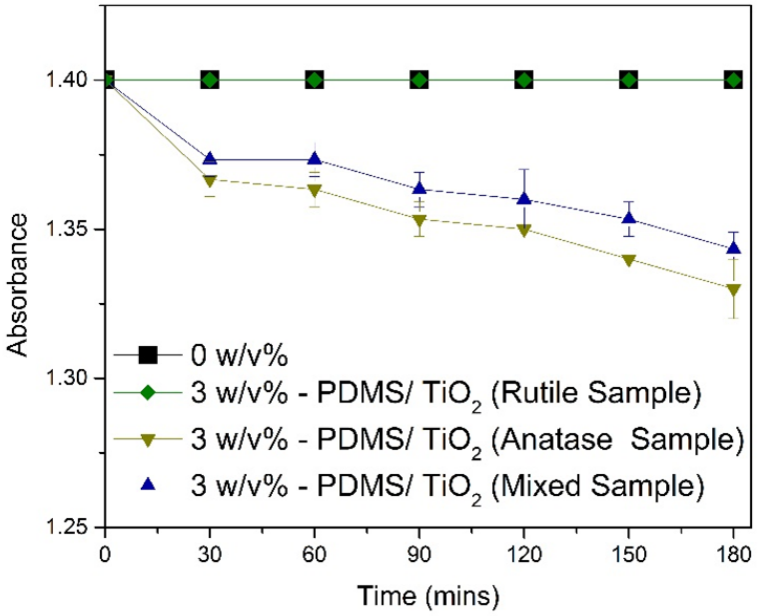

and the broader absorption gap that the anatase phase has in comparison to the rutile phase. However, while research directly comparing the phases based on the photocatalytic effects of unloaded TiO_2 NMs has been carried out (Farbod & Khademalrasool, 2011; Liao & Liao, 2007), research on the photocatalytic influence of the TiO_2 NM phase within nanocomposite coatings is limited.

Surface Stability

The coatings' durability was tested by subjecting the samples to accelerated UV exposure for seven days. After exposure, the WCA measurements of the samples, as shown in Figure 11, decreased by an average of $1° \pm 0.95°$ when compared to their original WCA. This decrease in WCA is attributed to the chain scission that is experienced by the PDMS in the presence of UV. This involves both the main backbone and the side-groups (Efimenko et al., 2002). However, all samples retained a WCA higher than 90°, confirming that hydrophobicity was not compromised. This indicated that although there are very minimal signs of degradation, the coatings are still considered durable to withstand UV radiation. From the four samples tested, the anatase phase PDMS/TiO_2 coating showed the least reduction in WCA.

The samples exposed to UV for seven days also had their photocatalytic performance reassessed. Only the anatase phase samples loaded with 3 w/v% TiO_2 NMs were chosen for this test as previously these showed the greatest photocatalytic activity, as shown in Figure 10, and therefore were believed to be the most promising. From the results obtained, as seen in Figure 12, a similar trend to that exhibited before the 7-day accelerated UV exposure was observed, as shown in Figure 14 in the Appendix. Furthermore, a marginal improvement in the photocatalytic ability of the samples after accelerated UV exposure was noted as time progressed. This could be due to some of the outer layers of the PDMS matrix being broken down, further explaining the reduction in WCA, as seen in Figure 11. This could have led to exposing more of the TiO_2 NM, leading to less inhibition of their photocatalytic effect by the PDMS. The radicals formed when UV is incident on PDMS can recombine, forming a network whose wetting properties are close to those of a pure PDMS (Efimenko et al., 2002). This helps shed light on the WCA similarities before and after UV exposure.

Figure 11. Average WCA measurements with error bars representing the standard deviation of each set of PDMS/TiO_2 coated samples (0, 0.6, 1, & 3 w/v%) before and after the 7-day UV exposure

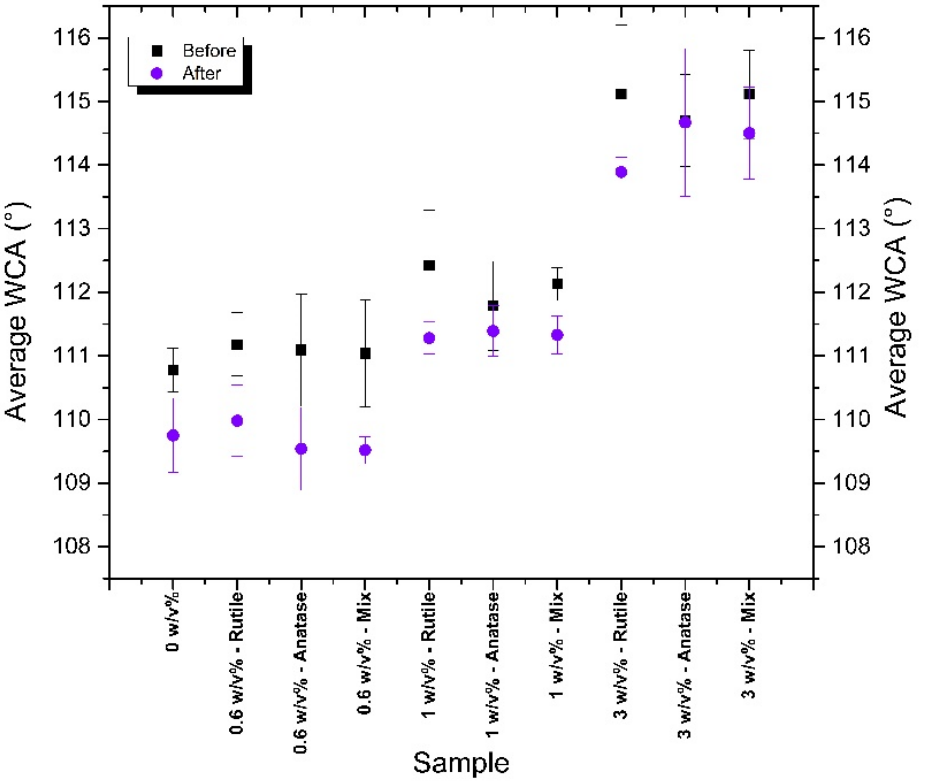

Figure 12. Absorbance of methylene blue at 664 nm over time for the anatase phase 3 w/v% PDMS/TiO_2 nanocomposite coatings

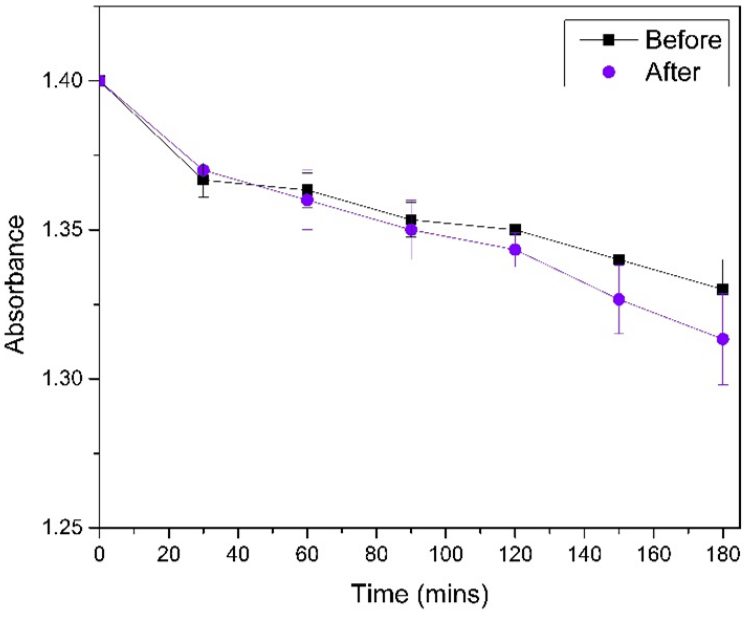

CONCLUSION

In this work, PDMS/TiO_2 self-cleaning coatings were developed, where a variation of both the TiO_2 NMs phase and concentration were investigated to determine the most effective and efficient combination. From the results obtained, the anatase phase was found to exhibit the greatest photocatalytic effect out of the three samples (anatase, rutile, and mixed) tested. Furthermore, the PDMS/TiO_2 anatase phase nanocomposite coating with a 3 w/v% TiO_2 NM concentration showed promising photocatalytic effects and indicated self-cleaning ability as well as a good surface stability when exposed to accelerated ageing by UV irradiation, with the photocatalytic activity being further enhanced.

ACKNOWLEDGMENT

The authors are also grateful for the support of Prof E. Valsami-Jones from the University of Birmingham for providing the NMs from JRC.

COMPETING INTERESTS

The authors declare that there are no competing interests.

FUNDING

The authors acknowledge financial support from University of Malta Research SEED Fund.

REFERENCES

Adachi, T., Latthe, S. S., Gosavi, S. W., Roy, N., Suzuki, N., Ikari, H., Kato, K., Katsumata, K., Nakata, K., Furudate, M., Inoue, T., Kondo, T., Yuasa, M., Fujishima, A., & Terashima, C. (2018). Photocatalytic, superhydrophilic, self-cleaning TiO2 coating on cheap, light-weight, flexible polycarbonate substrates. *Applied Surface Science*, *458*, 917–923. doi:10.1016/j.apsusc.2018.07.172

Ali, M. K. A., Xianjun, H., Elagouz, A., Essa, F. A., & Abdelkareem, M. A. A. (2016). Minimizing of the boundary friction coefficient in automotive engines using Al2O3 and TiO_2 nanoparticles. *Journal of Nanoparticle Research*, *18*(12), 377. Advance online publication. doi:10.1007/s11051-016-3679-4

Aresta, A., Calvano, C. D., Trapani, A., Cellamare, S., Zambonin, C. G., & De Giglio, E. (2013). Development and analytical characterization of vitamin(s)-loaded chitosan nanoparticles for potential food packaging applications. *Journal of Nanoparticle Research*, *15*(4), 1592. Advance online publication. doi:10.1007/s11051-013-1592-7

Augustynski, J. (1993). The role of the surface intermediates in the photoelectrochemical behaviour of anatase and rutile TiO_2. *Electrochimica Acta*, *38*(1), 43–46. doi:10.1016/0013-4686(93)80008-N

Banerjee, S., Dionysiou, D. D., & Pillai, S. C. (2015). Self-cleaning applications of TiO_2 by photo-induced hydrophilicity and photocatalysis. *Applied Catalysis B: Environmental*, *176–177*, 396–428. doi:10.1016/j.apcatb.2015.03.058

Benedix, R., Dehn, F., Quaas, J., & Orgass, M. (2000). Application of titanium dioxide photocatalysis to create self-cleaning building materials. *Lacer*, 157–168.

Bourikas, K., Kordulis, C., & Lycourghiotis, A. (2014). Titanium dioxide (anatase and rutile): Surface chemistry, liquid-solid interface chemistry, and scientific synthesis of supported catalysts. *Chemical Reviews*, *114*(19), 9754–9823. doi:10.1021/cr300230q PMID:25253646

British Standards. (2017). *ISO - ISO 10678:2010 - Fine ceramics (advanced ceramics, advanced technical ceramics) — Determination of photocatalytic activity of surfaces in an aqueous medium by degradation of methylene blue.* International Standard.

Chemin, J. B., Bulou, S., Baba, K., Fontaine, C., Sindzingre, T., Boscher, N. D., & Choquet, P. (2018). Transparent anti-fogging and self-cleaning TiO2/SiO2 thin films on polymer substrates using atmospheric plasma. *Scientific Reports*, *8*(1), 1–8. doi:10.1038/s41598-018-27526-7 PMID:29311619

Coelho, M. C., Torräo, G., Emami, N., & Grácio, J. (2012). Nanotechnology in automotive industry: Research strategy and trends for the future-small objects, big impacts. *Journal of Nanoscience and Nanotechnology*, *12*(8), 6621–6630. doi:10.1166/jnn.2012.4573 PMID:22962798

Coster, H. G. L. (2003). Chapter 2 dielectric and electrical properties of lipid bilayers in relation to their structure. Membrane Science and Technology, 7, 75–108. doi:10.1016/S0927-5193(03)80026-8

Dréno, B., Alexis, A., Chuberre, B., & Marinovich, M. (2019). Safety of titanium dioxide nanoparticles in cosmetics. *Journal of the European Academy of Dermatology and Venereology*, *33*(S7), 34–46. doi:10.1111/jdv.15943 PMID:31588611

Efimenko, K., Wallace, W., & Genzer, J. (2002). Surface modification of Sylgard-184 Poly (dimethyl siloxane) networks by ultraviolet and ultraviolet/ozone treatment. *Journal of Colloid and Interface Science*.

Farbod, M., & Khademalrasool, M. (2011). Synthesis of TiO2 nanoparticles by a combined sol-gel ball milling method and investigation of nanoparticle size effect on their photocatalytic activities. *Powder Technology*, *214*(3), 344–348. doi:10.1016/j.powtec.2011.08.026

Fujishima, A., Zhang, X., & Tryk, D. A. (2008). TiO_2 photocatalysis and related surface phenomena. *Surface Science Reports*, *63*(12), 515–582. doi:10.1016/j.surfrep.2008.10.001

Gale, B., Eddings, M. A., Sundberg, S., Hatch, A., Kim, J., Ho, T., & Karazi, S. (2016). Low-Cost MEMS Technologies. In Reference Module in Materials Science and Materials Engineering. doi:10.1016/B978-0-12-803581-8.00530-0

Garlisi, C., & Palmisano, G. (2017). Radiation-free superhydrophilic and antifogging properties of e-beam evaporated TiO_2 films on glass. *Applied Surface Science*, *420*, 83–93. doi:10.1016/j.apsusc.2017.05.077

Hadi Yousefi, M., Mahdi Zerafat, M., Shokri Doodeji, M., & Sabbaghi, S. (2017). Investigation of dip-coating parameters effect on the performance of alumina-polydimethylsiloxane nanofiltration membranes for desalination. *J. Water Environ. Nanotechnol*, *2*(4), 235–242. doi:10.22090/jwent.2017.04.002

Haider, A. J., Jameel, Z. N., & Al-Hussaini, I. H. M. (2019). Review on: Titanium Dioxide Applications. *Energy Procedia*, *157*, 17–29. doi:10.1016/j.egypro.2018.11.159

Imran, M., Riaz, S., & Naseem, S. (2015). Synthesis and characterization of titania nanoparticles by Sol-gel technique. *Materials Today: Proceedings*, *2*(10), 5455–5461. doi:10.1016/j.matpr.2015.11.069

Jain, A., & Vaya, D. (2017). Photocatalytic activity of TiO2 nanomaterial. *Journal of the Chilean Chemical Society*, *62*(4), 3683–3690. doi:10.4067/s0717-97072017000403683

Jang, H. D., Kim, S. K., & Kim, S. J. (2001). Effect of particle size and phase composition of titanium dioxide nanoparticles on the photocatalytic properties. *Journal of Nanoparticle Research*, *3*(2–3), 141–147. doi:10.1023/A:1017948330363

Kovacs, G. J., & Vincett, P. S. (1985). Particles in polymers: Surface chemistry of their nucleation, growth, configuration, and interactions with the matrix. *Canadian Journal of Chemistry*, *63*(1), 196–203. doi:10.1139/v85-031

Kumar, N., Yadav, S., Mittal, A., & Kumari, K. (2021). 15 - Photocatalysis by zinc oxide-based nanomaterials. In K. Awasthi (Ed.), *Nanostructured zinc oxide* (pp. 393–457). Elsevier. doi:10.1016/B978-0-12-818900-9.00005-X

Lan, Y., Lu, Y., & Ren, Z. (2013). Mini review on photocatalysis of titanium dioxide nanoparticles and their solar applications. *Nano Energy*, *2*(5), 1031–1045. doi:10.1016/j.nanoen.2013.04.002

Liao, D. L., & Liao, B. Q. (2007). Shape, size and photocatalytic activity control of TiO_2 nanoparticles with surfactants. *Journal of Photochemistry and Photobiology A Chemistry*, *187*(2–3), 363–369. doi:10.1016/j.jphotochem.2006.11.003

Linden, K. G., & Mohseni, M. (2014). 2.8 - Advanced oxidation processes: Applications in drinking water treatment. In S. Ahuja (Ed.), *Comprehensive water quality and purification* (pp. 148–172). Elsevier. doi:10.1016/B978-0-12-382182-9.00031-1

Magdassi, S., Grouchko, M., & Kamyshny, A. (2010). Copper nanoparticles for printed electronics: Routes towards achieving oxidation stability. *Materials (Basel)*, *3*(9), 4626–4638. doi:10.3390/ma3094626 PMID:28883344

Meng, F., Xu, Y., Wu, Z., & Chen, H. (2022). Transparent and superhydrophilic antifogging coatings constructed by poly (N-hydroxyethyl acrylamide) composites. *Colloids and Surfaces. A, Physicochemical and Engineering Aspects*, *642*, 128724. doi:10.1016/j.colsurfa.2022.128724

Moura, L., & Picão, R. C. (2022). Removal of antimicrobial resistance determinants from wastewater: A risk perspective on conventional and emerging technologies. In H. Sarma, D. C. Dominguez, & W. Y. Lee (Eds.), *Emerging contaminants in the environment* (pp. 603–642). Elsevier. doi:10.1016/B978-0-323-85160-2.00023-8

Nakata, K., & Fujishima, A. (2012). TiO_2 photocatalysis: Design and applications. *Journal of Photochemistry and Photobiology C, Photochemistry Reviews*, *13*(3), 169–189. doi:10.1016/j.jphotochemrev.2012.06.001

Nam, Y., Lim, J. H., Ko, K. C., & Lee, J. Y. (2019). Photocatalytic activity of TiO2 nanoparticles: A theoretical aspect. *Journal of Materials Chemistry. A, Materials for Energy and Sustainability*, *7*(23), 13833–13859. doi:10.1039/C9TA03385H

Nasimi, P., & Haidari, M. (2013). Medical use of nanoparticles: Drug delivery and diagnosis diseases. *International Journal of Green Nanotechnology*, *5*(1), 1–5. doi:10.1177/1943089213506978

Panutumrong, P., Metanawin, S., & Metanawin, T. (2015). The effect of nano-titanium dioxide on the self-cleaning properties of TiO_2-PP composite fibers. *International Journal of Advanced Culture Technology*, *3*(2), 25–33. doi:10.17703/IJACT.2015.3.2.25

Parkin, I. P., & Palgrave, R. G. (2005). Self-cleaning coatings. *Journal of Materials Chemistry*, *15*(17), 1689–1695. doi:10.1039/b412803f

Pathakoti, K., Manubolu, M., & Hwang, H. M. (2018). Nanotechnology applications for environmental industry. In Handbook of nanomaterials for industrial applications. Elsevier. doi:10.1016/B978-0-12-813351-4.00050-X

Racovita, A. D. (2022). Titanium dioxide: Structure, impact, and toxicity. *International Journal of Environmental Research and Public Health*, *19*(9), 5681. Advance online publication. doi:10.3390/ijerph19095681 PMID:35565075

Ragesh, P., Anand Ganesh, V., Nair, S. V., & Nair, A. S. (2014). A review on 'self-cleaning and multifunctional materials.'. *Journal of Materials Chemistry. A, Materials for Energy and Sustainability*, *2*(36), 14773–14797. doi:10.1039/C4TA02542C

Rai, A., Comune, M., & Ferreira, L. (2019). Nanoparticle-based drug delivery systems: Promising approaches against bacterial infections. *Antibacterial Drug Discovery to Combat MDR: Natural Compounds. Nanotechnology and Novel Synthetic Sources*, *57*, 605–633. doi:10.1007/978-981-13-9871-1_27

Rios, P. F., Dodiuk, H., & Kenig, S. (2009). Self-cleaning coatings. *Surface Engineering*, *25*(2), 89–92. doi:10.1179/174329409X373710

Sakthivel, S., Hidalgo, M. C., Bahnemann, D. W., Geissen, S. U., Murugesan, V., & Vogelpohl, A. (2006). A fine route to tune the photocatalytic activity of TiO2. *Applied Catalysis B: Environmental*, *63*(1), 31–40. doi:10.1016/j.apcatb.2005.08.011

Shafaamri, A., Cheng, C. H., Wonnie Ma, I. A., Baig, S. B., Kasi, R., Subramaniam, R., & Balakrishnan, V. (2020). Effects of TiO_2 nanoparticles on the overall performance and corrosion protection ability of neat epoxy and PDMS modified epoxy coating systems. *Frontiers in Materials*, *6*, 336. Advance online publication. doi:10.3389/fmats.2019.00336

Shafique, M., & Luo, X. (2019). Nanotechnology in transportation vehicles: An overview of its applications, environmental, health and safety concerns. *Materials (Basel)*, *12*(15), 11–17. doi:10.3390/ma12152493 PMID:31390752

Silva-Bermudez, P., & Rodil, S. E. (2013). An overview of protein adsorption on metal oxide coatings for biomedical implants. *Surface and Coatings Technology*, *233*, 147–158. doi:10.1016/j.surfcoat.2013.04.028

Singh, T., Shukla, S., Kumar, P., Wahla, V., Bajpai, V. K., & Rather, I. A. (2017). Application of nanotechnology in food science: Perception and overview. *Frontiers in Microbiology*, *8*, 1–7. doi:10.3389/fmicb.2017.01501 PMID:28824605

Strauss, M., Pastorello, M., Sigoli, F. A., Silva, J. M. S., & Mazali, I. O. (2014). Singular effect of crystallite size on the charge carrier generation and photocatalytic activity of nano-TiO2. *Applied Surface Science*, *319*, 151–157. doi:10.1016/j.apsusc.2014.06.071

Syafiq, A., Vengadaesvaran, B., Ahmed, U., Rahim, N. A., Pandey, A. K., Bushroa, A. R., Ramesh, K., & Ramesh, S. (2020). Facile synthesize of transparent hydrophobic nano-$CaCO_3$ based coatings for self-cleaning and anti-fogging. *Materials Chemistry and Physics*, *239*, 121913. doi:10.1016/j.matchemphys.2019.121913

Syafiq, A., Vengadaesvaran, B., Pandey, A. K., & Abd Rahim, N. (2018). Superhydrophilic smart coating for self-cleaning application on glass substrate. *Journal of Nanomaterials*, *2018*, 1–10. Advance online publication. doi:10.1155/2018/6412601

Syafiq, A., Vengadaesvaran, B., Rahim, N. A., Pandey, A. K., Bushroa, A. R., Ramesh, K., & Ramesh, S. (2019). Transparent self-cleaning coating of modified polydimethylsiloxane (PDMS) for real outdoor application. *Progress in Organic Coatings*, *131*, 232–239. doi:10.1016/j.porgcoat.2019.02.020

Tavares, M. T. S., Santos, A. S. F., Santos, I. M. G., Silva, M. R. S., Bomio, M. R. D., Longo, E., Paskocimas, C. A., & Motta, F. V. (2014). TiO2/PDMS nanocomposites for use on self-cleaning surfaces. *Surface and Coatings Technology*, *239*, 16–19. doi:10.1016/j.surfcoat.2013.11.009

Tayade, R. J., Surolia, P. K., Kulkarni, R. G., & Jasra, R. V. (2007). Photocatalytic degradation of dyes and organic contaminants in water using nanocrystalline anatase and rutile TiO_2. *Science and Technology of Advanced Materials*, *8*(6), 455–462. doi:10.1016/j.stam.2007.05.006

Tong, P., Sheng, Y., Hou, R., Iqbal, M., Chen, L., & Li, J. (2022). Recent progress on coatings of biomedical magnesium alloy. *Smart Materials in Medicine*, *3*, 104–116. doi:10.1016/j.smaim.2021.12.007

Vrakatseli, V., Farsari, E., & Mataras, D. (2020). Wetting properties of transparent anatase/rutile mixed phase glancing angle magnetron sputtered Nano-TiO_2 films. *Micromachines*, *11*(6), 616. Advance online publication. doi:10.3390/mi11060616 PMID:32630471

Wang, Y., Huang, Z., Gurney, R. S., & Liu, D. (2019). Superhydrophobic and photocatalytic PDMS/TiO2 coatings with environmental stability and multifunctionality. *Colloids and Surfaces. A, Physicochemical and Engineering Aspects*, *561*, 101–108. doi:10.1016/j.colsurfa.2018.10.054

Yasmina, M., Mourad, K., Mohammed, S. H., & Khaoula, C. (2014). Treatment heterogeneous photocatalysis; Factors influencing the photocatalytic degradation by TiO2. *Energy Procedia*, *50*, 559–566. doi:10.1016/j.egypro.2014.06.068

Zhao, W., & Lu, H. (2021). Self-cleaning performance of super-hydrophilic coatings for dust deposition reduction on solar photovoltaic cells. *Coatings*, *11*(9), 1–10. doi:10.3390/coatings11091059

APPENDIX

The appendix contains figures showing the decay curve trend lines for the photocatalytic activity results obtained from UV absorbance analysis of methylene blue.

Figure 13. Absorbance of methylene blue at 664 nm over time for each PDMS/TiO_2 coated sample along with decolourisation decay curves trend lines

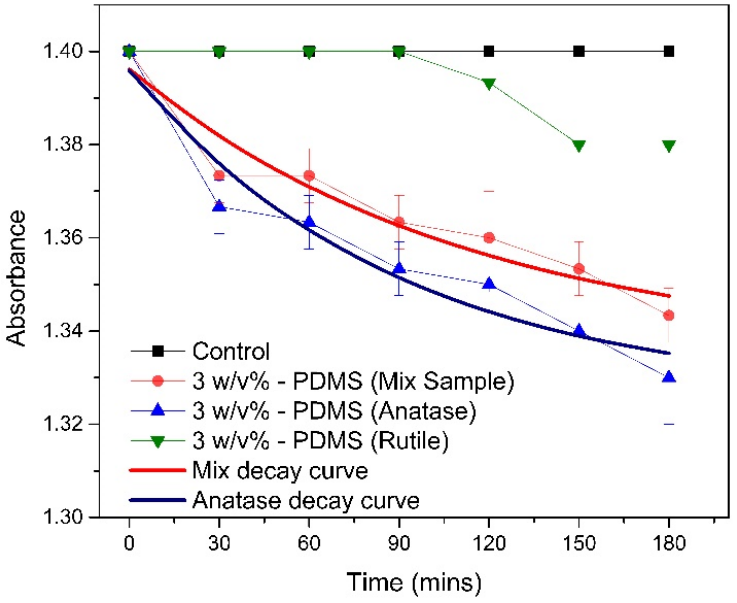

Figure 14. Absorbance of methylene blue at 664 nm over time for the anatase phased 3 w/v% PDMS/TiO_2 nanocomposite coatings fitted with decay trend lines